Energy Conversion and Management 286 (2023) 117070

Contents lists available at ScienceDirect

Energy Conversion and Management

journal homepage: www.elsevier.com/locate/enconman

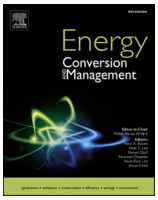

Multi-scale modelling of a fluidized bed biomass gasifier of industrial size (1 MW) using a detailed particle model coupled to CFD: Proof of feasibility and advantages over simplified approaches

Lukas von Berg [a,*], Andrés Anca-Couce [b], Christoph Hochenauer [a,c], Robert Scharler [a,c]

[a] Graz University of Technology, Institute of Thermal Engineering. Inffeldgasse 25/B, 8010 Graz, Austria
[b] Carlos III University of Madrid, Thermal and Fluids Engineering Department, Avda. de la Universidad 30, 28911 Leganés, Madrid, Spain
[c] BEST – Bioenergy and Sustainable Technologies GmbH, Inffeldgasse 21b, 8010 Graz, Austria

ARTICLE INFO

Keywords:
Multi-scale modelling
Particle model
CFD
Fluidized bed
Biomass
Gasification

ABSTRACT

Fluidized bed biomass gasification is a complex process whereby gas source terms are released by reactions at the particle level during the movement of fuel particles throughout the reactor. The current study presents for the first time the application of a multi-scale modelling approach for a fluidized bed biomass gasifier of industrial size, coupling a detailed one-dimensional particle model based on the progressive conversion model (PCM) with a commercial CFD software. Results of particle movement and gas source terms are compared with results of an additional simulation employing the simplified uniform conversion model (UCM) which is commonly used in literature. Validation at the particle level showed that the UCM leads to a massive underprediction of the time needed for pyrolysis whereas the PCM is in good agreement with experimental data. This heavily influences the gas sources released during pyrolysis of the biomass particles in the coupled reactor simulations. Volatiles are much more concentrated to the close proximity of the fuel feed when using the UCM whereas the PCM leads to a more homogeneous distribution over the reactor cross-section. The calculation time analysis of the coupled simulations showed that despite the increased complexity, the PCM shows only an increase of 20% in calculation time when compared to the UCM, whereas it is much better suited for these conditions. The coupled multi-scale simulations using the PCM showed the numerical feasibility of the modelling approach for 1,200,000 bed parcels and about 80,000 reacting fuel parcels and furthermore highlighted the importance of a comprehensive description of the particle level.

1. Introduction

The heavy reliance of humankind on fossil fuels is a major problem due to human-induced global warming [1] caused by CO_2 emitted through combustion of fossil fuels but also due to the dependency on few countries with large deposits of fossil fuels. Therefore, alternative energy sources need to be further developed and brought to market maturity in order to decrease the share of fossil fuels on our energy demand. Biomass can be used as a local and CO_2 neutral source of energy. Combustion of biomass is already a mature technology whereas biomass gasification is a promising conversion route that still needs further development to be commercially employed at bigger scale. Biomass gasification allows for a CO_2 neutral substitute of fossil fuels which can be employed to generate electricity (e.g. via a combustion motor [2] or a fuel cell [3]) or as a syngas to obtain various liquid or gaseous biofuels and chemical products [4,5].

Whereas several technologies have been developed for biomass gasification, fluidized bed reactors employing steam as fluidization medium are the most promising way to produce syngas from biomass at small and medium-scale [6] as they lead to a high quality nitrogen-free syngas. However, this technology comes with the difficulty of supplying the reactor with energy to keep the endothermic gasification reactions running. Different concepts have been designed to overcome this difficulty whereas the dual fluidized bed technology is strongly represented

Abbreviations: CFD, Computational fluid dynamics; CR, Combustion reactor; CV, Control volume; DDPM, Dense discrete phase model; DEM, Discrete element method; GR, Gasification reactor; KTGF, Kinetic theory of granular flow; MP-PIC, Multiphase particle-in-cell; PCM, Progressive conversion model; SR, Steam reformation; TC, Tar cracking; TFM, Two-fluid model; UCM, Uniform conversion model; WBRC, Woodland biomass research centre; WGS, Water gas shift.

* Corresponding author.
E-mail address: lukas.vonberg@tugraz.at (L. von Berg).

https://doi.org/10.1016/j.enconman.2023.117070
Received 14 February 2023; Received in revised form 5 April 2023; Accepted 15 April 2023
Available online 22 April 2023

in current research and industry [6–8]. Thereby, a bubbling fluidized bed gasifier is combined with a circulating fluidized bed combustor whereas the bed material acts as a heat carrier between the two reactors. However, the combination of complex fluid dynamics, intra-particle gradients and the complicated gas phase kinetics make it difficult to fully understand and optimize such a facility [9]. Therefore, a coupled multi-scale modelling tool combining a detailed description of the reactor level and the particle level is necessary to get a profound overview of the relevant processes and thereby support the development of this technology.

As shown in the review by Gomez-Barea and Leckner [10], various modelling approaches for fluidized bed biomass gasification have been developed in the past. Besides the more basic (however still very useful) approaches, the most commonly used modelling strategy today is based on computational fluid dynamics (CFD) which is becoming more and more feasible with increasing computing power. In general, CFD modelling of the reactor-scale of fluidized beds can be divided into two main categories [11]. The reactor level can either be described using the two-fluid model (TFM), also referred to as Euler-Euler approach or multi fluid model. Thereby, both the gaseous as well as the solid phase are represented by two interpenetrating continua. The other common approach to describe the reactor level is based on the Euler-Lagrange framework, where the gaseous phase is treated in the Eulerian description whereas the tracks of individual particles are described using the Lagrange description. When modelling the collisions of particles in the Euler-Lagrange framework, there are two main strategies. The discrete element method (DEM) allows for a realistic description of particle collisions but is not well suited for large facilities as its computational demand is very high as extremely small time-steps are needed to resolve particle collisions. Nevertheless, this approach is increasingly being used for lab-scale FBBG plants as it allows for a very precise description of the particle movements and can provide essential insights into the behaviour on the particle scale [12]. The hybrid Euler-Lagrange approach (e.g. the MP-PIC in MFIX or the DDPM in ANSYS Fluent) allows for a more efficient way to approximate particle collisions by using the kinetic theory of granular flow (KTGF). An additional advantage of the Euler-Lagrange approach is the possibility to group several particles in so called parcels to further reduce the computational demand. Overall, the combination of the Euler-Lagrange approach using approximated particle collisions combined with clustered particles represents an attractive trade-off between accuracy and computation time, even for industrial fluidized bed systems, and is therefore widely used in the literature [13,14]. Furthermore, compared to the TFM, this approach allows to track the conversion of individual particles along their movement through the reactor and is therefore well suited to be combined with a particle model.

The processes at the particle level during biomass gasification span from heat-up and drying to pyrolysis until the remaining solid char is gasified. Depending on the conditions in the particle, a simplified model for particle conversion may be used. In order to assess the thermal heat transfer regime, the Biot number can be used. It is defined as the ratio of thermal resistance inside the particle (conduction) compared to the thermal resistance at the particle surface (heat transfer). The Biot number predicts a thermally thin behaviour with negligible temperature gradients inside the particle for $Bi < 0.1$ and a thermally thick behaviour where gradients in temperature and conversion need to be considered for $Bi > 0.1$ [9]. Analysis of the Biot number of typical biomass particles (0.1–10 mm) in fluidized bed conditions indicates a thermal behaviour in the transition region or a thermal thick behaviour which requires a comprehensive particle model resolving intra-particle gradients [9,15]. A review of biomass gasification modelling by Safarian et al. [16] emphasizes that a combination of detailed kinetics with accurate fluid dynamic modelling is necessary to be able to describe the conditions in fluidized bed reactors. Furthermore, the review paper of Alobaid et al. [17] on CFD simulations of fluidized bed reactors emphasizes the importance of combining a comprehensive particle model considering intra-particle gradients with a detailed description of the gas flow and the particle movement for future work. As shown in the study by Ostermeier et al. [18], several modelling studies in literature use CFD approaches to model pilot-scale fluidized bed biomass gasification plants, but almost all of them use highly simplified models to describe the particle scale neglecting gradients in the particle [19,20]. This clearly shows the lack of comprehensive multi-scale models which employ a detailed description of the particle scale for a reactor of relevant size and is the main motivation of this study.

A recent review paper of Luo et al. [9] investigated the particle models commonly used for CFD modelling of fluidized bed biomass pyrolysis. Although focused on biomass pyrolysis, the study of Luo et al. [9] is of high interest for biomass gasification as pyrolysis is a main step of biomass gasification and highly relevant for tar formation. A detailed description of pyrolysis and tar formation for future modelling studies of biomass gasification is furthermore emphasized by Safarian et al. [16]. The most frequently used model in recent literature is the uniform conversion model (UCM). This model is widely used due to its simplicity and low computational cost and allows for straightforward implementation into the CFD framework. However, it is only suited for the thermally thin regime as it overestimates the pyrolysis rate for typical biomass particles which show thermally thick behaviour [9]. The review paper of Lu et al. [21] furthermore states that coupled CFD-UCM models need to consider a scaling factor to adapt for the overprediction of the pyrolysis rate when used for thermally thick particles. This scaling factor needs calibration when used for different particle size and shape which significantly limits the flexibility of the approach. A comprehensive description of the thermally thick biomass particles can be achieved by using a progressive conversion model (PCM) which allows to describe the conversion throughout the particle while considering intra-particle gradients. Usually a 1D description of the particle is used assuming an isotropic spherical particle [9]. However, such models typically show a high computational effort especially when coupled to CFD where boundary conditions for the reacting particles are constantly changing [22]. Furthermore, a coupling can only be realized with the Euler-Lagrange CFD approach and is moreover hindered by the extremely high number of reacting particles in a fluidized bed. A comparison of these two particle modelling approaches suited for multi-scale simulations is shown in Fig. 1. The reactor level described with CFD can be coupled with the PCM, which leads to a more detailed description of the particle level at the expense of a higher computational effort, or with the simplified and comparatively fast UCM, which, however, has only limited applicability in the case of biomass conversion.

There are a few studies using a particle description based on the PCM combined with CFD. However, all of these studies presented in [9] are modelling small lab scale units. Furthermore, they are either conducted with a 2D-CFD description or employ the highly computational demanding DEM approach to describe particle interactions which makes them hardly feasible to model larger plants. For example, Gao et al. [23] modelled biomass pyrolysis in a packed bed reactor with a 1D model coupled to the DEM solver of MFiX and showed that the intra-particle effects cannot be neglected in their case. A further study of Gao et al. [24] uses a coupled approach to model an entrained flow reactor by coupling a 1D particle model with a detailed biomass pyrolysis kinetic scheme to the MP-PIC model in MFiX. In their study, they found that the isothermal model lead to better results than the more complex non-isothermal model which might be related to the kinetics that already partially include intraparticle transport, hindering the applicability of this approach.

The multi-scale modelling approach for fluidized bed reactors developed by our research group is presented in the study of von Berg et al. [25]. It was shown that coupling a hybrid Euler-Lagrange CFD model based on the DDPM in ANSYS Fluent (resolving the reactor scale) with a detailed model describing the conversion at the particle level using a one-dimensional PCM is feasible for a very small 1.5 kW lab-scale bubbling fluidized bed reactor. Short calculation times were

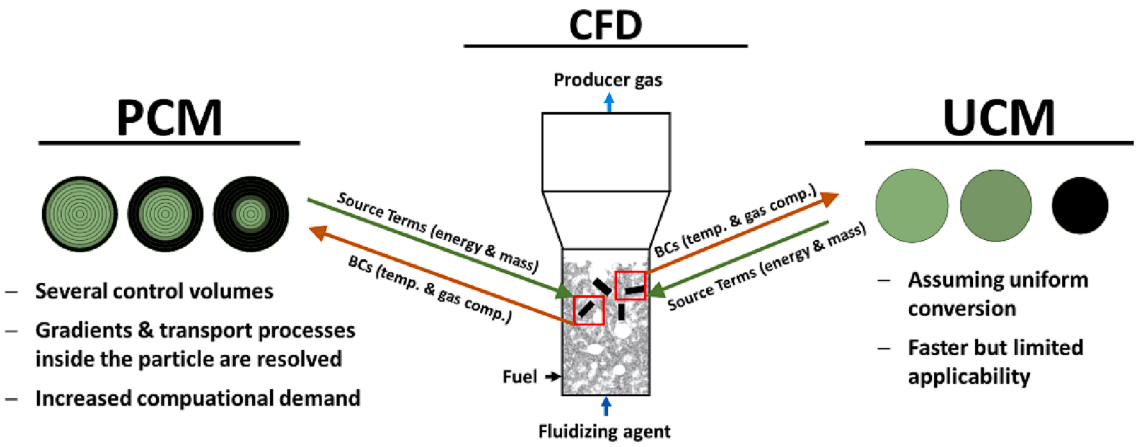

Fig. 1. Multi-scale modelling approaches investigated in the current study. A CFD approach to describe the reactor level (centre) is either combined with a PCM approach (left) or a UCM approach (right) for the particle level.

achieved by combining an optimized solver developed for the particle model by Anca-Couce and Zobel [22] with a time-saving initialization routine using partly converted biomass particles which allows to quickly reach a constant state in the reactor. An analysis of calculation time conducted in the study showed encouraging estimates that this coupled multi-scale model can also be successfully applied for larger plants with feasible computational effort. However, the feasibility of applying such a model on a scale of industrial relevance has yet to be demonstrated.

In the current study, we show for the first time the feasibility to model a 1 MW gasification pilot plant using a multi-scale CFD-PCM approach, going beyond previous lab scale studies. While the modelling approach in this study is similar to that in our previous publication, in the current study we go significantly further by applying a multi-scale model with a detailed one-dimensional description of the particle level for the first time on an industrial scale, while assessing the computational requirements. Therefore, the proof of feasibility shown in the current study is very relevant for a meaningful application of the model, as the high computational demand is one of the major obstacles and the main reason why these models are very scarce in the literature. The influence of simplification through the use of an UCM for the particle scale is investigated, assessing the need and feasibility of employing a detailed particle model based on the PCM in a plant of relevant size. Therefore, the coupled modelling approach employing a detailed PCM for the particle scale [25] is used to model the 1 MW thermal power dual fluidized bed biomass gasification pilot plant at Woodland Biomass Research Centre (WBRC) [26] whereas only the gasification reactor of the plant is investigated. Modelling results will be compared to available experimental data. An additional simulation is conducted using the simpler UCM approach for the particle scale but with exactly the same settings for the reactor scale allowing for a detailed comparison between a coupled multi-scale model based on the UCM or the PCM. The effects of increased complexity of the PCM over the UCM are discussed and a comparison of calculation time is conducted.

2. Numerical modelling

The modelling approach applied in this study is based on the DDPM implemented in the CFD software ANSYS Fluent (V2021 R2) which describes the gaseous and solid phase at the reactor level. This model was extended via user defined functions (UDF) by a particle model based on the PCM to describe biomass conversion including heat-up, drying, devolatilization and char gasification. Furthermore, a simplified particle model based on the UCM was implemented using UDFs. The two particle modelling approaches can furthermore be run as stand-alone simulations in order to evaluate and compare the influence of the particle model in an easy manner.

As the modelling approach is rather complex, a step-wise validation has been conducted in the past by our research group. Modelling of fluidized bed reactors has been investigated intensively by Blehrmühlhuber et al. [27] whereas the cold-flow models of the NETL [28] where used to validate the simulation results. Findings of this study are used as the basis of the reactor-scale modelling of the current study. The original version of the particle model was tested thoroughly by Anca-Couce et al. [29] using a single particle reactor. Adaptions of the particle model for conditions in a fluidized bed environment with a focus on heat transfer correlations were conducted by von Berg et al. [15] and validated using experimental results. A thorough investigation and validation of the individual models in simplified cases is necessary for a detailed assessment of the multi-scale modelling results and to better understand the influence of each model.

2.1. Reactor scale

To model the reactor scale, the dense discrete phase model (DDPM) implemented in ANSYS Fluent was chosen using the kinetic theory of granular flow (KTGF) to approximate particle collisions. When using the DDPM-KTGF, particle properties obtained via the Lagrangian description are interpolated to the Eulerian grid which allows to consider particle collisions in an efficient way using the KTGF.

For dense gas solid flows as in fluidized beds, the drag model by Gidaspow [30] is recommended [31]. More sophisticated models are developed recently which is especially important when using coarse grids [32] and particle clustering [33]. Most of these models are developed for the TFM framework [34–36], a few studies can be found where such models are adapted for the use in the DDPM framework [14]. However, the focus of our study is on the coupling procedure and the influence of the particle model and therefore, the Gidaspow model, which is well established for fluidized beds, was employed. The theory of the DDPM as well as a description of the KTGF together with the details of the sub-models can be found in the supplementary material. When employing the DDPM-KTGF, some limitations need to be considered. It was found that the particles show unphysical behaviour for gas velocities below the minimal fluidization velocity [25,37], where particles seem to overlap and accumulate at the gas distributor in a very shallow layer which can be relevant e.g. in the loop-seal when modelling a dual fluidized bed. Furthermore, the ratio of the parcel diameter to cell size is limited as problems can occur when too few parcels fit in a single cell [27]. For coarse meshes in large-scale fluidized beds, this is not a big problem but still needs to be considered especially when using particle clustering and when small geometry details need to be resolved.

The finite rate/eddy dissipation model [38] implemented in Fluent is used to account for homogeneous gas phase reactions. As shown in

Table 1
Homogeneous gas phase reactions (values in square brackets have units of kmol/m^3).

	Reaction	Reaction rate r in kmol / (m^3×s)	
Water gas shift [26]	$CO + H_2O \rightarrow CO_2 + H_2$	$r_{WGS} = 2.75 \times e^{\frac{8.38 \times 10^7}{RT}} [CO][H_2O]$	(R1)
Steam reformation [41]	$CH_4 + H_2O \rightarrow CO + 3H_2$	$r_{SR} = 5.92 \times 10^8 \times e^{\left(\frac{2.09 \times 10^8}{RT}\right)} [CH_4]^{0.5}[H_20]$	(R2)
Tar cracking [42]	$Tar \rightarrow 0.707H_2 + 1.054CO + 0.219CO_2 + 0.489CH_4 + 0.103C_6H_6$	$r_{TC} = 3.7 \times 10^7 \times e^{\left(\frac{1.19 \times 10^8}{RT}\right)} [Tar]$	(R3)

Table 1, water gas shift reaction, methane steam reformation and tar cracking are considered. As the tar content in the gas obtained via biomass gasification is still one of its main problems for many applications, a detailed description of the tar formation and cracking is very important as emphasized by Safarian et al. [16]. However, due to its complex nature, most CFD studies in literature use rather simplified approaches. The current study uses an advanced approach whereas the stoichiometric coefficients of the tar cracking reaction are based on the detailed RAC pyrolysis reaction scheme [29], in a similar way as done in the study of Scharler et al. [39] and employing detailed thermal tar cracking reactions proposed by Mellin et al. [40]. A more detailed description of this approach can be found in our previous publication [25]. The current approach is still a rather simplified description but allows to be easily adapted for future work e.g. by employing more tar species released from the particle model combined with additional tar cracking reactions in the gas phase.

2.2. Particle scale

The following section first discusses the differences between the two particle models which are subsequently coupled to the CFD simulation. Afterwards, modelling settings applied for both particle models in the same way are further explained.

2.2.1. PCM

The PCM model applied in this study is similar as the one in our previous study [25] based on the biomass pyrolysis model developed by Anca-Couce and Zobel [22]. The model uses a solving strategy optimized to allow for a fast solution when dealing with constantly changing boundary conditions as in a fluidized bed reactor. Usually applied solvers for particle models (like the ODE solver) show rather poor performance in such conditions due to the high computational demand for the initialization at each timestep. The model uses 10 control volumes (CV) over the radius which showed to lead to accurate results while not being too demanding regarding computational cost. Heat transfer is regarded via conduction and convection whereas transport of mass is considered via convection and diffusion. However, diffusion was only considered during gasification after 99 mass% of the volatiles where released during pyrolysis. Pyrolysis and gasification can be assumed to take place consecutively [43]. In the case of the particles used in this study pyrolysis is completely finished after 10 s whereas gasification takes more than 1000 s. Fick's law is used to model diffusion employing diffusion coefficients based on the Chapman-Enskog equation. Model settings used for both versions of the particle model as well as properties of the employed biomass are summarized in Table 2.

2.2.2. UCM

In order to compare the results of the detailed particle model with the UCM which is frequently used in literature, a simplified particle model using the UCM approach was furthermore employed. The main difference is the radial discretization inside the particle when using the PCM whereas the UCM cannot describe gradients inside the particle. This means that for the UCM, mass transport by convection and diffusion as well as heat transport by conduction and convection are not considered inside the particle.

Table 2
Parameters of the particle model and biomass properties.

Thermal conductivity biomass	0.177	W/(m×K)
Thermal conductivity char	0.1	W/(m×K)
Solid density	1500	kg/m^3
Minimum shrinkage factor	0.46	–
Heat capacity biomass	1500 + T	J/(kg×K)
Heat capacity char	420 + 2.09×T – 6.85×10^{-4} ×T^2	J/(kg×K)
Heat capacity water	4200	J/(kg×K)
Permeability biomass	1×10^{-14}	m^2
Permeability char	1×10^{-12}	m^2
Pore diameter	1×10^{-4}	m
Emissivity	0.9	–
Dynamic viscosity gas	1x10^{-5}	kg/(m×s)
Thermal conductivity gas	0.0258	W/(m×K)

2.2.3. Chemical reactions employed for the PCM and UCM

The particle model employed for biomass gasification considers drying, pyrolysis and gasification with H_2O and CO_2 as presented in Table 3. Furthermore, shrinkage is considered during biomass conversion. The PCM uses the local temperature and concentration in each CV to calculate the reaction rates in each CV whereas the UCM uses the mean value of the particle.

A first-order Arrhenius equation [44] is used to model drying according to reaction (R4). A single-step global reaction scheme is used to describe pyrolysis as shown in reaction (R5) using the kinetics given in [44]. The pyrolysis reaction mechanism is derived from the detailed RAC mechanism by Anca-Couce et al. [29] which is based on the mechanism of Ranzi et al. [46]. This detailed model is used to obtain the stoichiometric coefficients of the simplified mechanism for char, permanent gases as well as a lumped tar species by running a simulation with boundary conditions representative for the investigated case. This approach allows for a fast calculation based on a detailed description of pyrolysis and is furthermore very flexible when planning to increase the complexity e.g. for a more detailed description of tar by employing several tar compounds. Char gasification is considered via H_2O (R6) and CO_2 (R7) using the kinetics by Van de Steene et al. [45]. More details can be found in [25].

2.2.4. Boundary conditions of the PCM and UCM

Special attention must be paid to boundary conditions for particles in a fluidized bed reactor and heat and mass transfer correlations especially derived for these conditions are available in literature. In a previous study of our research group [15], heat transfer correlations for large biomass particles in a fluidized bed of hot sand were evaluated. It was shown that models that include the effect of fluidization velocity are better suited for a broader range of operating conditions. Therefore, the model of Agarwal [47] was used in the present study. Mass transfer was considered using the Sherwood number calculated as $Sh = 2\varepsilon + 0.69(Re_p/\varepsilon)^{1/2}Sc^{1/3}$ as given in [48] for fluidized bed conditions. Thereby ε is the void fraction, Re_p is the particle Reynolds number and Sc is the Schmidt number, all calculated based on the conditions of the corresponding CFD cell. Heat and mass transfer coefficient

Table 3
Heterogeneous reactions and applied kinetics (values in square brackets have units of kg/m^3).

	Reaction	Reaction rate r in kg / (m^3×s)	
Drying [44]	$H_2O(l) \rightarrow H_2O(g)$	$r_{drying} = 5.56 \times 10^6 \times e^{-87.9\times10^3 / (R\times T_{CV})}[H_2O]_{CV}$	(R4)
Pyrolysis [44]	$Biomass(s) \rightarrow Char(s) + CO + H_2O + CO_2 + H_2 + CH_4 + Tar$	$r_{pyrolysis} = 2.0 \times 10^8 \times e^{-133.1\times10^3 / (R\times T_{CV})}[Biomass]_{CV}$	(R5)
CO_2 gasification [45]	$Char(s) + CO_2 \rightarrow 2CO + (\frac{\alpha_C}{2} - \beta_C)H_2 + \beta_C H_2O + Ash(s)$	See reference	(R6)
H_2O gasification [45]	$Char(s) + (1 - \beta_C)H_2O \rightarrow CO + (1 + \alpha_C/2 - \beta_C)H_2 + Ash(s)$	See reference	(R7)

calculated via Nusselt and Sherwood number are then employed in the outermost CV of the PCM and for the UCM to consider heat and mass transfer. Furthermore, radiation is considered in the particle model. The particle model is solved at every fluid time-step for each individual particle considering the corresponding boundary conditions (gas temperature, gas composition and gas velocity) and source terms for gas species and energy are forwarded to the CFD-cell where the particle is currently located. Results of the particle model that are required for the solution of the next timestep are stored for every particle. The new particle temperature, density, mass and diameter calculated by the particle model are updated for each corresponding particle in the reactor model. This procedure can also be conducted when using parcels (representing several particles) in the CFD framework, whereas the source terms released by the particle model need to be scaled accordingly.

3. Experimental rig and modelling settings

The coupled multi-scale model was validated using experimental data of the 1 MW thermal dual fluidized bed gasifier located at Woodland Biomass research centre (WBRC) in California, USA [26]. As shown in Fig. 2.a, the WBRC pilot plant consists of a bubbling bed gasification reactor (GR, shown in blue) and a combustion reactor (CR, shown in red) operated as a riser. A chute at the bottom of the GR where particles are led to the CR combined with a loop seal which allows for the hot bed material to be fed back to the GR leads to a circulation of bed material between the two reactors. In the current study, only the gasification reactor was investigated in order to evaluate the importance of detailed particle modelling during biomass gasification. When modelling the full-loop of a circulating fluidized bed reactor, several zones with different particle flow regimes are present in the domain. The gasifier is operated as a bubbling bed, the loop seals and pipes connecting the reactor have a very dense particle flow whereas the combustion reactor shows a dilute particle flow. As it is difficult to describe these effects all at once using the DDPM, especially when the packing limit is reached, we choose to only model the gasifier in order to focus on the effect of the influence of the particle model. The gasification reactor has a total height of about 6 m and consists of a conically shaped bottom part and a cylindrical freeboard with a diameter of about 1 m.

Fuel is fed to the GR from the side of the reactor in the lower part of the bubbling bed and steam fed from the bottom of the reactor is used as fluidizing agent. Part of the bed material as well as partly converted biomass particles leave the GR through a chute in the bottom part of the bubbling bed at the opposite site of the fuel feed leading to the CR. The producer gas outlet is located at the top of the GR highlighted in pink. Experimental gas composition at the reactor outlet are available. The operating conditions of the experimental case modelled in this work are

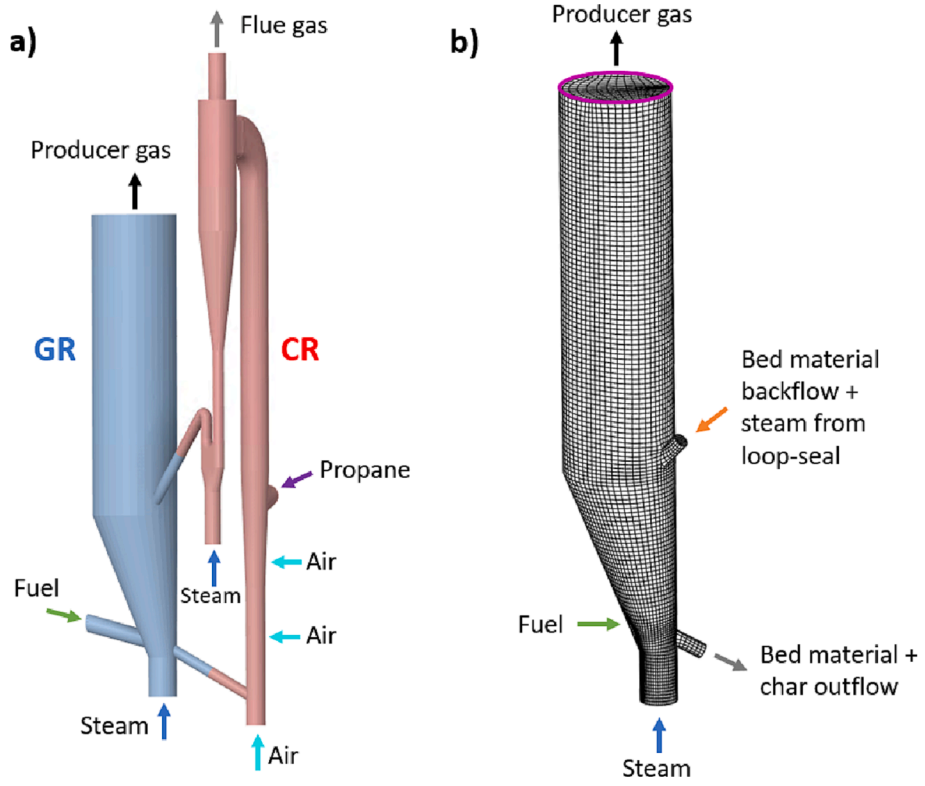

Fig. 2. Scheme of the experimental rig (a) and CFD mesh of the reactor geometry of the gasifier with boundary conditions for gas and solid flow (b).

presented in the study by Liu et al. [26] as "Case 2". The operation conditions and further input for the simulation in this study are presented in Table 4. Almond pruning with a moisture content of about 5 % and a density of 554 kg/m^3 was employed as fuel. As detailed properties for almond pruning for e.g. thermal conductivity or heat capacity are not available in literature, representative values for similar biomass was employed [25]. Modelling was conducted assuming spherical particle shape with a mean diameter of 5.7 mm as given in [26].

3.1. Simulation setup

The multi-scale simulation was set up in ANSYS Fluent 2021 R2 as a transient simulation with a fluid time-step of 0.0001 s. The default values of Fluent were used for residuals (1e-3 for all equations except for energy where the limit is 1e-6) while about 10 to 15 iterations where necessary to reach the convergence criteria for each timestep. The mesh of 43,438 cells used to represent the geometry of the gasifier was generated based on the recommendations and best practice guidelines by ANSYS Fluent [50] for the DDPM and is shown in Fig. 2.b. The DDPM-KTGF model in Fluent is employed to describe the reactor level. Due to the limitations of the DDPM, a finer mesh is not suitable as the cell size must be sufficiently larger than the parcel size. In general, however, the DDPM shows much better grid independence when compared to the TFM, as the Lagrangian particle tracking leads to a much more accurate representation of the volume fraction as shown by Cloete et al. [51]. The TFM, on the other hand, suffers from significant numerical diffusion and cannot resolve distinct volume fraction gradients when using coarse meshes [51]. A primary phase is defined representing the gas phase and a granular phase is introduced to represent the particulate matter. Thereby, the clustering concept is utilized to reduce the computational demand whereas 1,200,000 bed parcels are considered to represent the bed material. Furthermore, biomass particles are clustered whereas one biomass parcel represents 4 real particles, allowing for a faster solution of the particle scale while still respecting the limitations of parcel size compared to the cell size of the mesh. This leads to about 75,000 biomass parcels. The particle model uses the same time-step as the fluid-scale. More information about the sub-models employed for the DDPM-KTGF can be found in Table 5. The DDPM-KTGF settings are the same as in our previous work [25], however, the current study also considers radiation based on the *P*1 model including the effect of particles on the absorption coefficient.

As only the gasification reactor is modelled in the current study, several assumptions needed to be made. It is supposed that the char led to the combustor is totally burned as indicated by several studies [6,57,58]. The hot bed material is then completely recirculated to the gasifier via a loop seal, whereas the particles are assumed to have the same temperature as the gas temperature at the combustor outlet. Benedikt et al. [59] state that the temperature of the bed material leaving the combustion reactor has approximately the same temperature as in the top of the combustion reactor for their 100 kW dual-fluidized bed biomass gasification pilot plant, which backs this assumption. For our study, the temperature measured at the outlet of the combustion reactor during the experiments is 1207 K [26] which is used as the backflow temperature of the bed material. A further assumption has to be made assuming the steam flow fed to the loop seal whereas we assume that it is evenly distributed to the GR and the CR. The bed material recirculation rate of the WBRC gasifier was investigated by Liu et al. [49] in a numerical study whereas a recirculation rate of 5.44 kg/s is given for similar conditions as employed in the current study. The recirculation of particles was implemented using a UDF whereas bed material particles close to the chute at the gasifier bottom are relocated to the backflow position in the upper part of the gasifier while respecting the given recirculation rate. The temperature of the relocated bed material particles is set to 1207 K. Furthermore, biomass or char particles located in the chute to the combustor are detected and removed from the domain.

In total, two coupled CFD simulations were conducted in this study. One simulation employs the CFD settings shown above coupled with the comprehensive PCM as a particle model via a UDF. The other simulation uses the exact same CFD settings for the reactor level, however, it is coupled with the simplified particle model based on the UCM via a UDF. Therefore, the only difference of the two simulations is the description of the particle level which however will strongly influence source terms released at the reactor scale.

Table 4
Operating conditions and model input derived from the experimental case [26].

Biomass feed rate	220	kg/h
Biomass diameter	0.0057	m
Initial biomass temperature	293	K
Biomass particle density (wet)	554	kg/m^3
Biomass moisture content (as received)	5	%
Gasifier steam feed rate	78	kg/h
Temperature of steam flow to gasifier	603	K
Total steam supply to loop-seal (of which 50 % goes to the GR)	85 (42.5 to GR)	kg/h
Bed material recirculation rate [49]	5.44	kg/s
Bed material backflow temperature	1207	K

Table 5
Models and sub-models employed for the CFD simulations.

Property	Employed model
Multiphase model	DDPM
Particle interactions	KTGF
Radiation	P1 (0 bands – grey gas approximation)
Turbulence model	Standard k-ε model (enhanced wall treatment)
Transition factor	0.65
Drag law	Gidaspow [30]
Granular viscosity	Syamlal and O'Brien [52]
Granular bulk viscosity	Lun et al. [53]
Solid pressure	Lun et al. [53]
Granular temperature	Algebraic
Frictional viscosity	Schaeffer [54]
Frictional pressure	Johnson and Jackson [55]
Friction packing limit	0.5
Angle of internal friction	30
Packing limit	0.52
Radial distribution function	Ma Ahmadi [56]
Specularity coefficient	0.5
Solid wall boundary condition	Johnson and Jackson [55]
Solid-solid restitution coefficient	0.8
Particle emissivity	0.9
Particle scattering factor	0.9

3.2. Boundary conditions and initialization

The operation conditions of the experiments presented in [26] were used to derive the boundary conditions of the CFD simulation (see Table 4). The steam-flow rate at the gas distributor is set to 78 kg/h. A fixed temperature of 1123 K was set on the reactor wall according to the mean temperature of the gasifier during the experiments as due to the vigorous mixing inside the bed, a similar temperature at the wall can be assumed. This allows for a good estimation, however, more detailed information about the insulation of the reactor wall would allow to use a heat-flux boundary condition which would probably allow to better describe the temperature in the reactor. The constant wall temperature used in this study does not consider temperature differences along the reactor height which might occur due to different insulation, the high heat capacity of the bed in the lower part of the bed as well as the effect of the backflow of hot bed material. The boundary condition on the wall is set to a no-slip condition for the gas phase and to a partial-slip condition for the discrete phase according to Johnson and Jackson [55]. The specularity coefficient describes the effect of friction between particle and wall whereas a value of 0 represents a no-slip condition and a value

between 0 and 1 represents partial slip. In the current study, it was set to 0.3, close to the value of 0.1 recommended for denser fluidization conditions [60]. For all walls, it was specified that particles are reflected. This setting was also chosen for the syngas outlet as it is located at the very top of the freeboard and particles will not be very likely to be transported in this area due to the smooth bubbling behaviour of the gasification reactor. The particle outlet at the bottom of the gasifier is treated as a wall whereas the connection to the loop-seal in the upper part is realized as a mass-flow inlet to respect the steam flow coming from the loop seal. Both interfaces between gasifier and combustor are set to show reflective behaviour for particles since the recirculation rate of the particles was respected using a UDF as described above.

In order to quickly reach a constant operating point during the transient simulation, an advanced initialization routine was conducted to account for an initial char bed in the gasifier. The conversion of a single biomass particle at the operation condition of the gasifier was investigated with the standalone version of each of the two single particle models. Whereas pyrolysis is finished after no more than 10 s, the following gasification of the residual char takes over 1000 s (see also Fig. 4). Therefore, there are usually a great amount of semi-converted char particles inside the bed which need to be considered. In our previous study modelling a lab-scale bubbling fluidized bed reactor [25], an initial char bed with biomass particles at different states of conversion was introduced at the beginning of the simulation based on results of a standalone particle model. However, in a circulating fluidized bed like in the present study, part of the char is burned in the combustor. Therefore, the conversion-time of a char particle is furthermore determined by how long it resides in the gasifier. Considering the recirculation rate of the plant and the total mass of bed material, a complete recirculation of the bed can be assumed in about 300 s. Due to the flotsam behaviour of char [61], it will be preferably located in the upper part of the bed and it is difficult to say if the char is recirculated in the same way as the bed material. Kraft et al. [62] state that smaller char particles are better mixed within the bed and therefore show a higher concentration in the recirculation stream compared to bigger ones. An elemental balance of the gasification reactor showed that for the investigated experimental case, about 40 % of the char react in the gasifier whereas the other 60 % are burned in the combustor. This shows the same trend as the findings of Liu et al. [26] who concluded that with this experimental setup, the char is primarily burned in the combustor whereas a smaller part is gasified. To determine the initial char bed in the gasifier of this study, the standalone particle model was used to calculate results for particles at different states of conversion using a representative temperature and gas composition. The results were stored using the time interval between two particles respecting the fuel feeding rate of the gasifier. Results of the standalone particle model necessary to continue the conversion calculation later on in the coupled calculation were stored at different grades of conversion. This resulted in a solution of the single particle model for each biomass particle that is fed to the reactor whereas the sum of these particles represents the char mass that would be in the gasifier if it was not partly combusted. As stated above, 60 % of the char are combusted. Therefore, only 40 % of the mass of all these particles at different states of conversion need to be considered in the initial char bed of the gasifier. Furthermore, with the information that small particles are more likely to be transported to the combustion reactor, we considered only the particles with shorter residence time (corresponding to a lower degree of conversion and a larger particle size) until 40 mass% char were reached. The particle with the highest degree of conversion determined by this method shows a residence time of 295 and 309 s for the UCM and PCM, which matches well with the time of full-recirculation of the bed material of 300 s. This results in an initial char bed consisting of partly converted biomass whereas it is assumed that 60 mass% of the char is already burned in the combustor. This procedure was conducted for both different particle models and led to 77,000 initial fuel parcels for the PCM and 73,700 fuel parcels for the UCM when using 4 particles per parcel.

The step-wise initialization procedure of each simulation starts with the injection of the bed material. Afterwards, the initial fuel bed is injected using the results at different states of conversion obtained by the standalone particle model. Thereby, the composition of the gas phase and the solid phase as well as the temperature in each control volume of the particle are patched to the corresponding parcel via a UDF. This step is followed by the continuous injection of fresh biomass according to the biomass feed rate. From there on, the particle model is solved for each fuel parcel at every time step whereas the boundary conditions in the corresponding CFD-cell are considered and source terms of the particle model are forwarded to the CFD simulation. After the gas composition at the outlet gets constant after about 20 s, the results are averaged for 10 s, resulting in a total simulation time of 30 s.

4. Results and discussion

First, the difference between the two particle modelling approaches based on the PCM and the UCM are investigated using the standalone version of each model. Afterwards, the results of the coupled multi-scale simulations are compared.

4.1. Comparison of the PCM and UCM based on the standalone particle model

To evaluate the influence of the different modelling approaches for the particle level, this section compares results based on standalone calculations using the PCM and the UCM. As stated in the study of Luo et al. [9], the UCM is commonly employed for fluidized bed biomass conversion neglecting the fact that it is not suitable for thermally thick particles showing gradients inside the particle. They furthermore state that the UCM overestimates the pyrolysis rate leading to a shorter overall conversion time. To investigate this phenomenon, the experimental results for biomass pyrolysis in a fluidized bed reactor presented by Wang et al. [63] are used to validate the two different particle modelling approaches. Pyrolysis experiments at 773 K employing beech wood cylinders of different diameter were conducted using nitrogen as fluidizing agent whereas the conversion time was analyzed. They conclude that for particles smaller than 2 mm, the process is kinetically controlled whereas for bigger particles, transport processes inside the particle need to be considered. Several simulations were set up using the experimental conditions of Wang for various particle diameters ranging from 0.5 to 16 mm, whereas each simulation was run with the PCM and the UCM. Thereby, the properties of Table 2 were employed while slight adaptions e.g. for the density were made to match the experimental conditions of Wang. The conversion time needed for pyrolysis determined by these simulations was defined as the time until 99 % of the volatiles were released, similar as in the study of Kersten et al. [64]. The comparison of conversion time for different biomass diameters between experimental results and modelling results using the PCM and the UCM are presented in Fig. 3. Good agreement is found between the experimental and the PCM modelling results. Pyrolysis times range from about 20 s for the very small particles to about 200 s for the biggest particle, which can be accurately predicted by the PCM. Modelling results based on the UCM show similar results as the PCM up to a diameter of 2 mm. However, the UCM predicts a faster conversion time for particles larger than 2 mm showing huge discrepancy with the experimental data. For particles of 6 mm diameter, which is the typical diameter of a biomass pellet, the PCM shows already a 46 % longer conversion time when compared to the UCM whereas this trend gets even stronger for bigger particles. This clearly shows the limits of applicability of the UCM for large biomass particles in fluidized bed reactors even at the considered moderate temperatures typical for fast pyrolysis. This result furthermore highlights the importance of a comprehensive particle model which resolves gradients inside the particle during pyrolysis for biomass especially for larger particles.

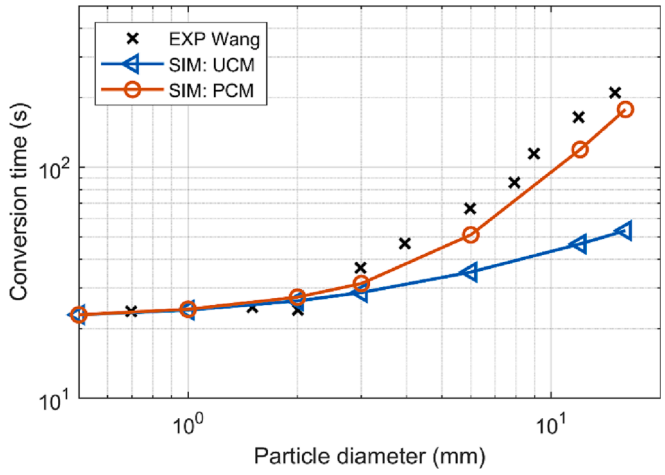

Fig. 3. Comparison of experimental results of conversion time of beech wood cylinders with 42 mm length and various diameter pyrolyzed at 773 K by Wang et al. [63] with modelling results based on the UCM (blue) and the PCM (orange).

4.2. Particle scale results at conditions of the WBRC gasifier

The following section will now investigate the behavior of the two particle models when applied to the conditions in the fluidized bed biomass gasification plant investigated in this study. Therefore, the standalone version of the PCM and the UCM was run using constant boundary conditions for temperature and gas composition representative for the investigated reactor. A comparison of the standalone modelling results of conversion is shown in Fig. 4. The diagram on the left shows the conversion during the first 15 s. For both models, pyrolysis is completed within a few seconds, as indicated by the plateau of the conversion curve, indicating that the heating, drying and pyrolysis of the particles are completed within this time. However, the UCM (blue) shows a much faster conversion during this period whereas it takes only 2.5 s until 99 % of pyrolysis is finished compared to 8.4 s for the PCM (orange). As shown above, the PCM shows good agreement with experimental data presented in literature also for larger biomass particles. Furthermore, the standalone PCM was already thoroughly validated in our previous study modelling fluidized bed biomass pyrolysis where good agreement with experimental data was achieved [15]. Therefore, the UCM significantly underestimates the time needed for pyrolysis at gasification conditions. As more than 80 % of the initial particle mass are released during this period, this can have a huge influence on the overall process as it will strongly influence at which location in the reactor the gas source terms are released during devolatilization when coupled to the reactor scale. The results clearly show the importance of a comprehensive particle model like the PCM when applied to typical conditions of fluidized bed biomass gasification.

The diagram at the right of Fig. 4 shows the time necessary for gasification of the residual char after pyrolysis, although the x-axis has a very different scale to that of the pyrolysis graph. Compared to pyrolysis, which is finished in a few seconds, gasification of the remaining char takes over 1300 s (about 22 min). When comparing the time needed for gasification, the UCM leads to a conversion time that is about 90 s faster when compared to the PCM, corresponding to about 6 %. This indicates that for the investigated particle size, the gasification of the remaining char can probably be described using a UCM with acceptable accuracy due to the much slower kinetics and much more homogeneous conditions inside the particle with rather small gradients during gasification [25]. However, the pyrolysis period previous to gasification has a significant impact on the gas obtained during the overall conversion in the gasifier whereas more than 80 % of the particle mass are released during this period. Furthermore, tar components are formed during pyrolysis which therefore needs to be accurately described.

4.3. Results of the coupled multi-scale model

To see the full effect of the influence of the particle model on the reactor scale, results of multi-scale simulations are investigated in the following section. Two coupled simulations were conducted employing the UCM on the one hand and the PCM on the other hand, whereas the reactor level was modelled using the same settings for both cases.

A snapshot of the position of particles after a time of 20 s is shown in Fig. 5 for both simulations. The results of the CFD-UCM simulation are shown in Fig. 5.a. The figure on the left shows the volume fraction of the bed material with typical behavior for a dense bubbling fluidized bed. A stream of recirculated particles is coming from the combustion reactor whereas the hot bed material particles are falling onto the top of the bubbling bed. A few gas bubbles can be seen rising from top to bottom in yellow as they show a lower packing density. However, most bubbles are located in the inner part of the reactor and cannot be seen in this view. Fig. 5.a on the right shows the density of the continuously fed biomass particles and of the initial char particles on the same scale. Fresh biomass particles with a density of about 550 kg/m^3 (red) are located only in the direct proximity of the fuel feed position. It seems that the very fast pyrolysis rates predicted by the UCM leads to devolatilization

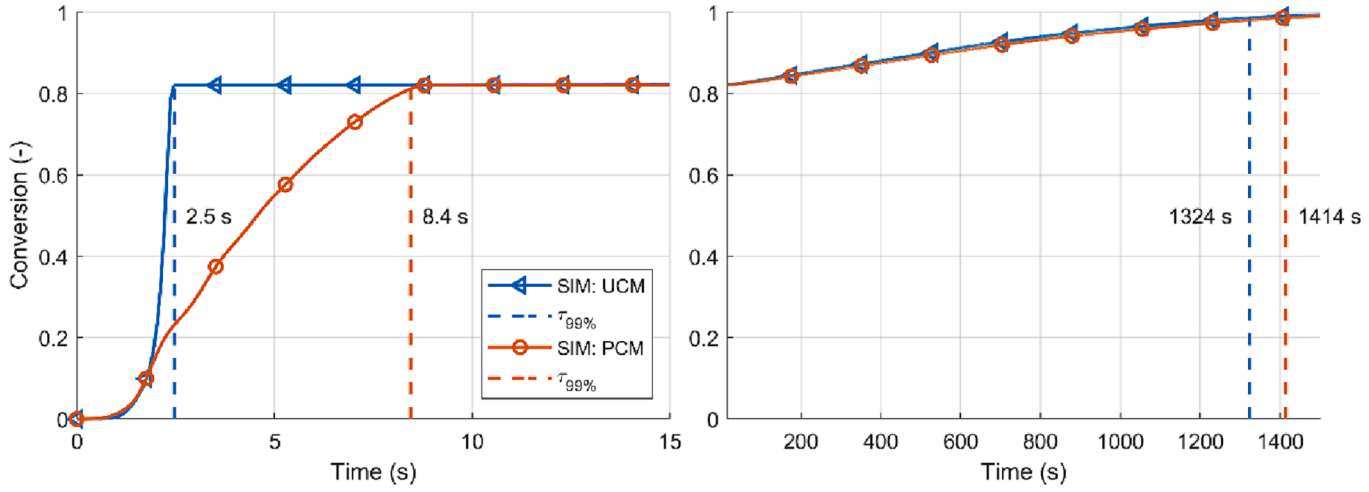

Fig. 4. Modelling results for conversion of a single particle at conditions of the reactor investigated in this study. The UCM predicts a pyrolysis time more than three times faster than the PCM (left). The differences between the two models during gasification are much smaller (right).

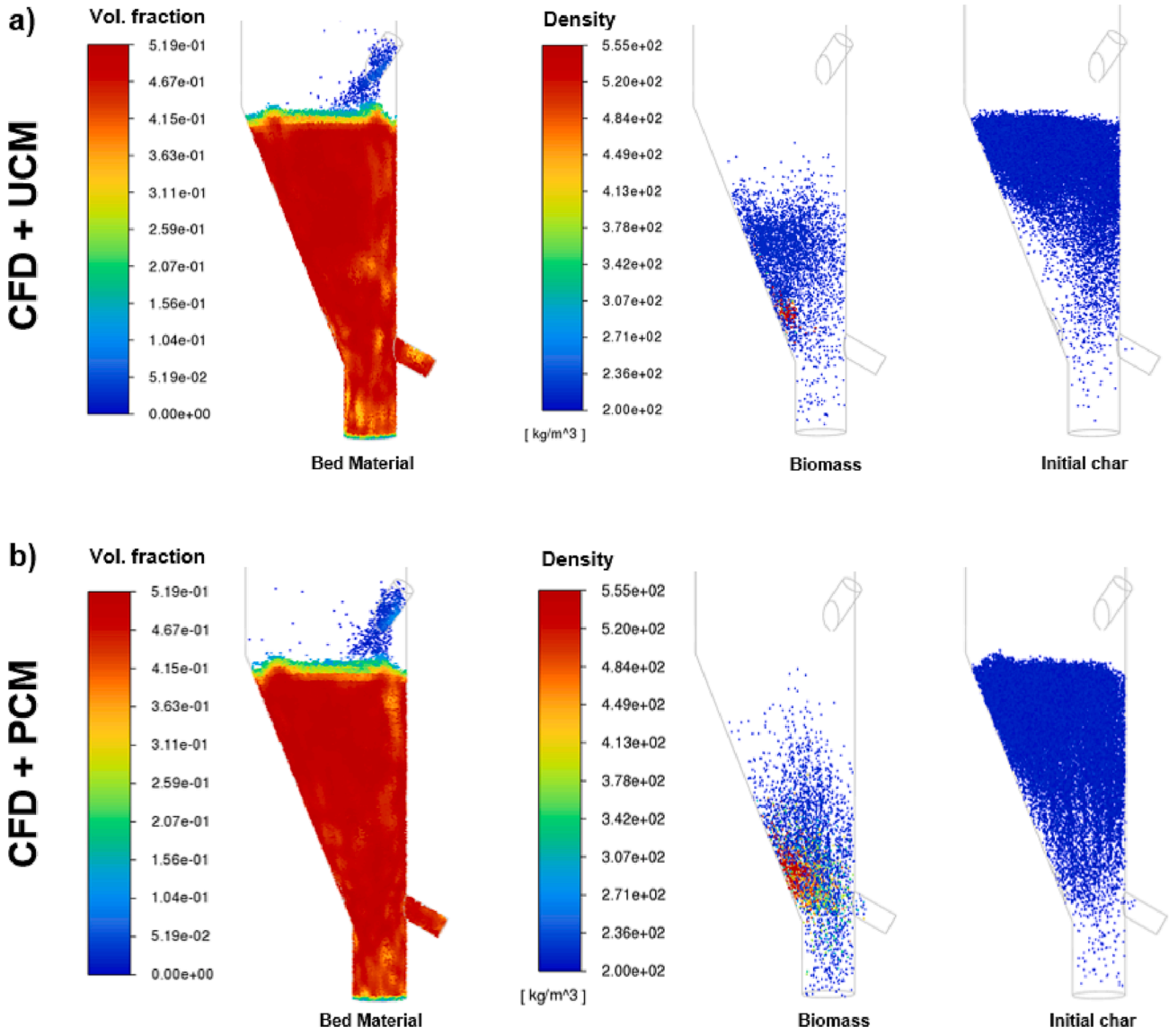

Fig. 5. Snapshot of volume fraction of the bed material (left) and density of the continuously fed biomass and initial char particles (right) after 20 s using the UCM (a) and PCM (b).

of the fuel particles before they are further mixed throughout the reactor. Pyrolysis is finished very quickly while particles are still close to the feeding position whereas the obtained char particles with a density close to 200 kg/m^3 (blue) resulting from the continuous biomass injection are mixed throughout the whole bed. When looking at the initial char on the very right of Fig. 5.a, the particles initially injected at the top of the bed are already well mixed with the bed material. However, at the proximity of the fuel feed, there seems to be a lower share of char particles which might be in conjunction with the high amount of volatiles released in this area resulting in an upward movement due to an increased bubbling intensity. A similar effect of a lower particle density at the close proximity of the fuel feed was found by Zhang et al. [65] when modelling air–steam gasification with a CFD-DEM using a simple particle model. However, in their case, the description of the particle level using the UCM is justified by the very small biomass particles which lead to very fast devolatilization rates close to the reactor feed. The same snapshots are shown for the PCM simulation in Fig. 5.b, whereas a similar distribution of bed material can be seen on the left-hand side of the figure. However, the distribution of the particles resulting from the continuous biomass injection and the initial char is clearly different. Looking at the density of the particles from the continuous biomass injection, there is a much larger area of pyrolyzing particles with a density between 200 and 555 kg/m^3. The distribution of char particles far right shows that when using the PCM, the char is evenly distributed over the whole cross-section of the reactor which is different when compared to the results obtained with the UCM.

For both models, the results show that biomass pyrolysis and devolatilization is happening while the particles are still located deep inside the bed which is advantageous as pyrolysis at the top of the bed can lead to increased methane and tar content of the producer gas [6]. The low-density char particles seem to be generally well mixed with the bed material whereas a slightly larger amount is accumulating on the top of the bed which can be beneficial as the char helps with the conversion of volatiles due to its catalytic effect [6]. Source terms related to char gasification are significantly lower when compared to the ones released during pyrolysis and are distributed much more evenly over the reactor due to the relatively homogeneous distribution of char in the bed. The modelling results showed a slight increase in the source terms for H_2 and CO at the top of the bed which can be attributed to the accumulation of char in this area of the bed due to the flotsam behaviour.

4.3.1. Particle tracks of reacting fuel particles

To better understand the movement of fresh biomass particles introduced in the lower part of the bed, the tracks of 10 representative particles were monitored during the coupled simulations. The particle tracks presented in Fig. 6 are shown from a side view (left) as well from the top (right) for both simulations whereas the location of the injection is marked with a yellow circle. The color gradient shows the residence time whereas for the two different simulations, the tracks where plotted until the end of pyrolysis corresponding to about 2.5 s for the UCM and 8.5 s for the PCM. The diameter of the markers is scaled with the diameter of the shrinking particle. Fig. 6.a shows the results of the coupled UCM simulation which clearly predicts that the pyrolyzing particles are rather close to the fuel feed point until they are fully pyrolyzed. This high concentration of devolatizing particles leads to a high release of gas source terms of the particle model in a rather small section of the reactor. In Fig. 6.b, the particle tracks of the coupled PCM simulation show that the pyrolyzing particles are distributed more evenly whereas the particles span over the whole cross-section at the height of the fuel feed. Whereas the total mass of gaseous source terms of the UCM and the PCM are the same, the big difference in conversion time predicted by each model leads to a very different distribution of source terms in the reactor when employed in a coupled simulation. These results highlight the importance of a multi-scale simulation where both particle scale and reactor level need to be described thoroughly in order to describe the interaction of the different scales.

The effect of the different distribution of the source terms between the two models is further analyzed in Fig. 7 showing the tar mass fraction in the reactor averaged between 25 and 30 s of simulation time. Fig. 7.a shows the results for the UCM which predicts a high concentration of about 30 % at the close proximity of the fuel feed as pyrolysis takes mainly place in this area. The tar mass fraction for the PCM presented in Fig. 7.b shows that tars are much more evenly distributed whereas the tar mass fraction is always below 10 %. For both simulations, the employed tar cracking kinetics lead to rather fast decrease of tar in the upper part of the bed and predict almost no tar species at the top of the bubbling bed. However, for future work with a stronger focus on modelling tar contaminants, it is essential to use the more accurate description of the release of tar species obtained with the PCM. As tar concentrations even at low levels significantly hamper the applicability of the product gas, a correct description of the tar release is essential to optimize biomass gasification.

4.3.2. Gas composition at the reactor outlet

After the transient simulation is started, it takes some time until the gas at the reactor outlet reaches a constant composition. However, compared to the time required to build up the char bed in the real plant, the initialization routine using an initial bed of fuel particles at various conversion states allows a constant state to be achieved in a very short time of about 20 s for both simulations. The evolution of the gas species at the reactor outlet is given in the supplementary material. In order to get averaged results, the simulation was run for another 10 s during which the gas composition was averaged over the outlet face of the

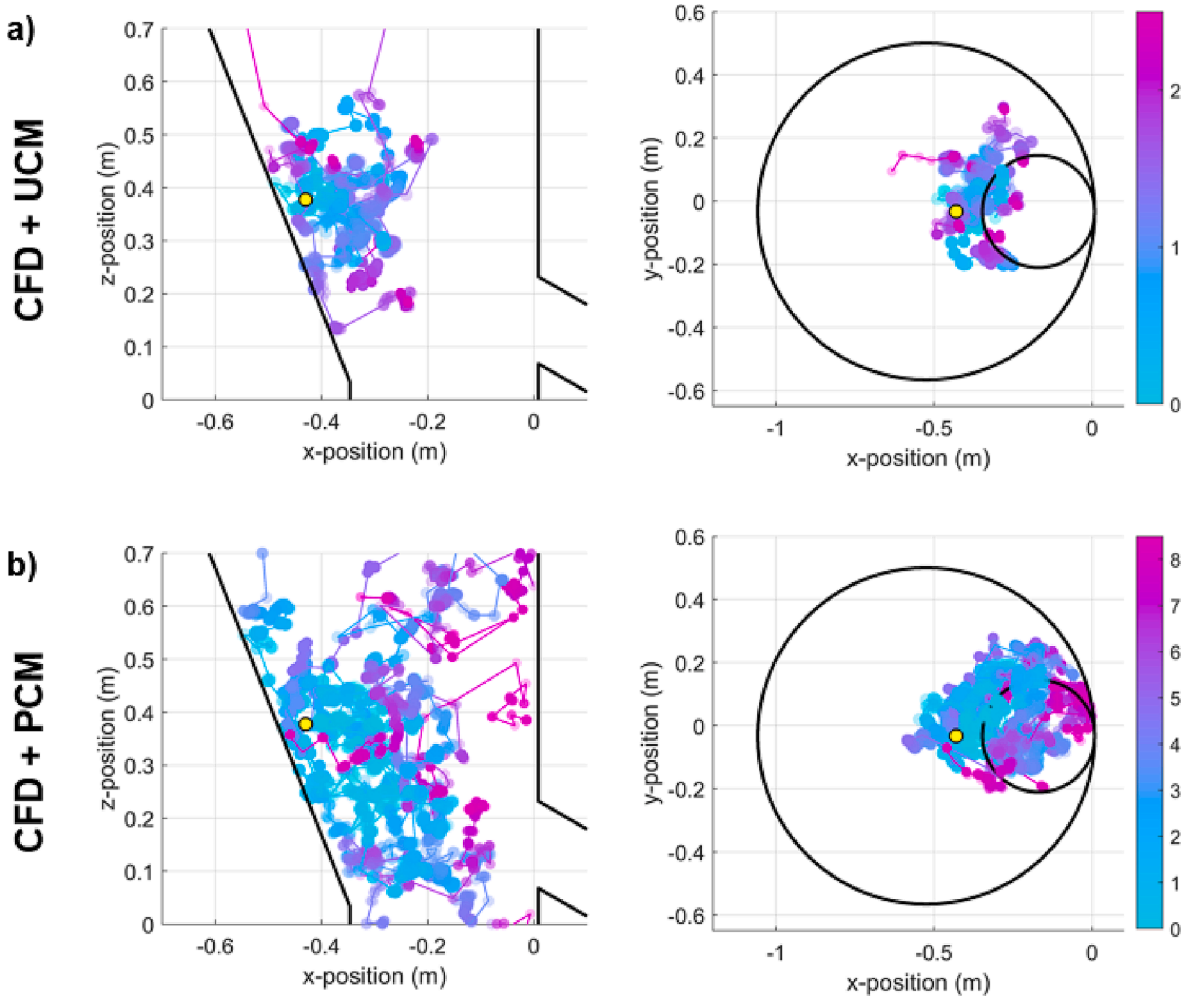

Fig. 6. Particle tracks of 10 representative biomass parcels during pyrolysis. For each model the tracks are plotted until the time when pyrolysis is finished corresponding to 2.5 s for the UCM (a) and 8.5 s for the PCM (b). The position of fuel injection is marked in yellow.

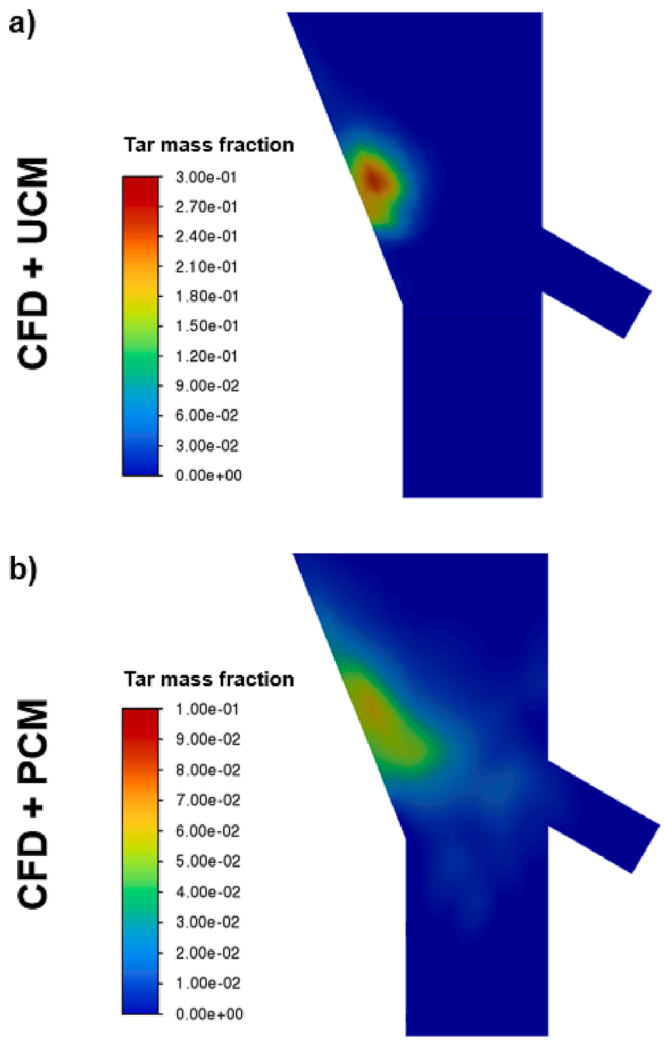

Fig. 7. Tar mass fraction (averaged from second 25 to 30 of the transient simulation) for the coupled simulation employing the UCM (a) and PCM (b).

geometry as shown in Fig. 2. A comparison of the average gas composition of both simulations with experimental results together with modelling results of Liu et al. [26] is shown in Fig. 8. The modelling results for the UCM and PCM show reasonable agreement with the experimental data except for CO and CO_2, which shows quite strong deviation for both simulations whereas CO is overpredicted and CO_2 is underpredicted. These deviations can primarily be related to the employed water gas shift kinetics. Compared to the modelling results obtained in our study, the modelling results of Liu et al. [26] presented in Fig. 8 show better agreement with experimental results. However, for their simulations, the kinetics were tuned to fit the experimental data. A tuning of kinetic parameters could be done in the future but was not conducted in the current study as it is outside of the scope of this work. The rather large share of benzene predicted by both simulations can be mainly attributed to the fact that the current model only considers primary tar cracking whereby benzene is produced. Secondary tar cracking should be included in future work. We showed that both models can generally predict the gas composition. However, the main difference between the results of the UCM and the PCM simulation is the position of the particles during pyrolysis where the major part of the gas release takes place which has a significant impact in the design of the reactor and in the final tar content. While the UCM can result in a similar permanent gas composition at the reactor outlet as the PCM, it cannot accurately describe the processes within the bed.

4.3.3. Analysis of calculation time

As computational feasibility is essential when developing new modelling approaches, the calculation time of the different particle models in combination with the reactor model was analyzed. Therefore, a third CFD simulation employing the DDPM was set up with same settings as the other two simulations but without employing a particle model to determine the computational demand of the DDPM (for this simulation, only the results regarding computational demand are discussed in this study). All simulations were run on a workstation equipped with an Intel® Core™ i9-10980XE CPU @ 3.0 GHz and 64 GB RAM running ANSYS Fluent 2021 R2 using 8 cores in parallel. All three simulations use 43,438 CFD cells and 1,200,000 bed parcels, whereas the coupled simulations employ 73,700 and 77,000 fuel parcels for the UCM and the PCM respectively. The total calculation time per time-step and the share of the different models is presented in Fig. 9. When not considering a particle model, the calculation time per time-step is just above 8 s, whereas 34 % of the time is necessary to solve the DDPM. The CFD-UCM model shows a total calculation time per time-step of about 9 s while about 8 % of the time is used to solve the UCM which shows the very low computational demand of this approach. The results of the CFD-PCM show that the overall time per time-step is about 11 s whereas the solution of the PCM takes about 25 % of the time. This shows that although the solution of the PCM takes almost 4 times longer than for the

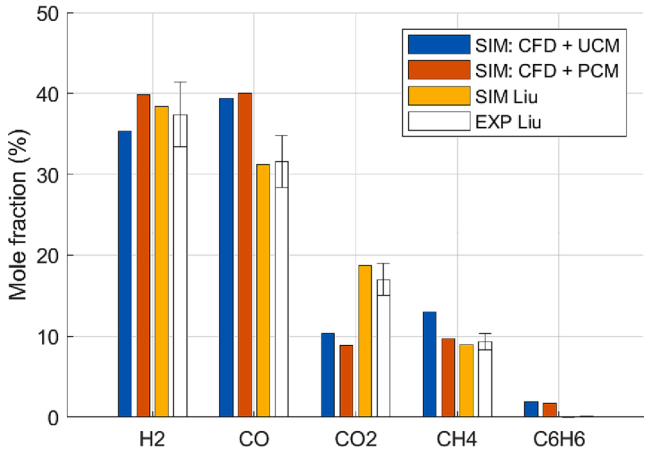

Fig. 8. Comparison of modelling results of gas composition at the gasifier outlet using the CFD-UCM and CFD-PCM with modelling and experimental results of Liu et al. [26].

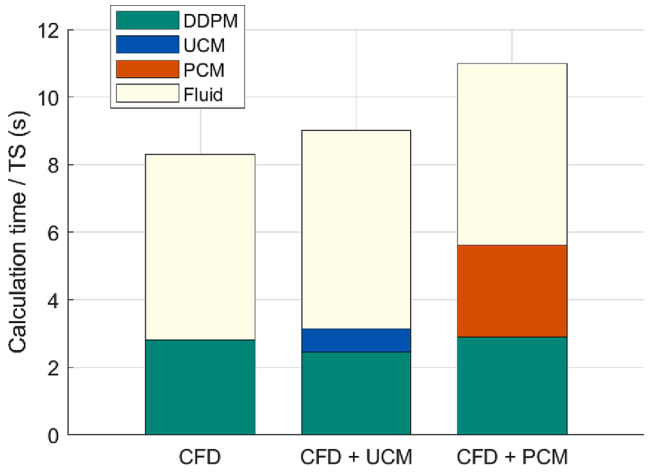

Fig. 9. Calculation time per time-step when using only the DDPM with non-reacting particles as well as for the multi-scale simulations coupled to a particle model.

UCM, the total time necessary to solve one time-step is only 22 % higher. The main computational demand of the coupled simulations can be related to the solution of the fluid phase and the particle movement. Therefore, the coupled CFD-PCM simulation allows for a much more accurate description of the particle scale while the computational demand is still feasible. In our previous publication about multi-scale modelling of a lab-scale fluidized bed gasifier [25], we predicted a rather optimistic share of only 2 % of calculation time for the particle model when modelling large scale plants. However, this prediction assumed that the bed material was clustered in the same way as for the lab-scale reactor studied at the time, which would result in an unacceptably high number of parcels for a large-scale reactor. In the lab-scale plant, the bed material was clustered using 110 particles per parcel whereas in the current study, one parcel represents 4980 bed particles. Therefore, in the current study, the relative share of the particle model is higher than predicted in the previous study. However, the overall time needed to solve a time-step is still lower than the initial expectations when developing this model and allows to further increase the complexity of the particle model and to implement more advanced description of tar for future modelling work. We were thus able to demonstrate for the first time that a multi-scale modeling approach employing a detailed description of the particle level can be applied for a large FBBG plant with acceptable computation times facilitated by an optimized solution approach for the particle model combined with an advanced initialization routine.

5. Conclusions

The current study aims to investigate the feasibility to employ a detailed particle model in a multi-scale approach coupled to a CFD software when modelling a pilot-scale fluidized bed biomass gasifier. The use of a particle model that resolves particle gradients combined with a reactor model that tracks individual particles has been called for in several recent review papers [16,17] on FBBG modelling. While our model was initially published modelling a small lab-scale gasifier (1.5 kW) with promising results regarding accuracy and computational demand [25], in the current paper, such a multi-scale modelling approach is applied for the first time in literature for a FBBG plant of industrial size (1 MW). The few multi-phase modelling approaches for FBBG that can be found in literature show to be very computational demanding and are usually only applied for very small reactors [9]. However, a comprehensive multi-scale model that can be applied at a larger scale is urgently needed in order to be able to use such a model in a meaningful way. Our current study is the first to demonstrate the feasibility of a detailed multi-scale model at an industrially relevant scale, making the model applicable to support the construction and optimization of real plants. Furthermore, the importance of a comprehensive description of the particle level is shown by comparing the results of the coupled CFD-PCM simulation with a CFD simulation employing a UCM model for the particle scale, which is commonly used in literature.

A validation of the detailed particle model based on the PCM and the simplified UCM with experimental data was conducted using standalone versions of each particle model to investigate their applicability. While similar results were achieved for very small, thermally thin particles with both models, the UCM leads to a strong deviation predicting a too fast pyrolysis rate for the particle size typically employed in fluidized bed biomass gasification. This clearly shows that the UCM is not applicable in typical FBBG conditions, even though almost all studies in literature are based on this simplified approach. Gasification of the remaining char is predicted in a similar way for both models, as for the investigated particle size, rather small gradients are present during gasification. However, the huge difference during pyrolysis when using the UCM and the PCM in combination with the particle movement leads to a rather different distribution of source terms at the reactor level when employing the two models in a multi-scale simulation. Especially for large reacting particles where gradients inside particles occur, the UCM leads to strong deviations and should not be used without a correction factor. These effects strongly influence the local concentration of gas species inside the reactor which is essential for the development and optimization of such a plant. This is especially relevant when, for instance, the tar concentration is investigated, which is crucial for biomass gasification. Therefore, the simplified approach using the UCM should not be used under such conditions as it predicts an incorrect gas distribution inside the reactor and can lead to misleading conclusions. When compared to the gases released during pyrolysis of the fresh biomass particles, source terms of char gasification are distributed much more evenly with a slight increase at the top of the bed correlating with the distribution of char particles in the reactor.

Experimental validation of such phenomena inside the reactor is difficult as the measurement of the required data in the bed is quite complex and can hardly be found in literature. Therefore, future experimental work should focus on more detailed measurement data necessary for the validation not only at the gasifier outlet but also inside the reactor. Nevertheless, the modelling results clearly show that the PCM is required to achieve an accurate description of the particle conversion inside the bed and it is very well suited to be coupled to the reactor scale with only a minor increase of calculation time of about 20 % when compared to the UCM. In this study, the feasibility to employ the PCM in a FBBG plant of relevant scale was shown for the first time while the deviations when using a simplified approach were investigated. Furthermore, the employed approach allows to further improve the description of the particle level via the implementation of more detailed chemistry in an easy manner. The detailed particle model has already been extensively tested for fluidized bed pyrolysis [15] and gasification [25], where it showed great flexibility and good agreement with experimental data. These promising results support a flexible application of the coupled multi-scale model at different operation conditions and when employing different feedstock in various gasification reactors in future work. The UCM is generally not suited to model FBBG as it cannot accurately describe biomass conversion at these conditions. It is possible to use a scaling factor to correct the error of the UCM. However, this scaling factor needs to be calibrated for different operating conditions as well as for different particle size and shape which makes this approach much less flexible. In combination with a more detailed description of tar cracking at the reactor level, this will allow to better describe the behavior of the tars in future modelling studies. Besides, the general structure and methodology of the developed approach can be employed for other fluidized bed technologies where particle gradients are relevant.

CRediT authorship contribution statement

Lukas von Berg: Conceptualization, Methodology, Software, Formal analysis, Investigation, Data curation, Writing – original draft. **Andrés Anca-Couce:** Methodology, Conceptualization, Supervision, Funding acquisition, Writing – review & editing. **Christoph Hochenauer:** Project administration, Supervision. **Robert Scharler:** Methodology, Conceptualization, Supervision, Funding acquisition, Writing – review & editing.

Declaration of Competing Interest

The authors declare that they have no known competing financial interests or personal relationships that could have appeared to influence the work reported in this paper.

Data availability

The data that has been used is confidential.

Acknowledgements

This project has received funding via the COMET Module BIO-LOOP (Austrian Research Promotion Agency Project Number 872189) which is funded by the Federal Ministry for Climate Action, Environment, Energy, Mobility, Innovation and Technology and the Federal Ministry for Digital and Economic Affairs as well as the federal province Styria. The COMET (Competence Centers for Excellent Technologies) programme is managed by FFG (Austrian Research Promotion Agency, www.ffg.at/comet). Further, we want to thank Reinhard Seiser for his support regarding questions about the reactor geometry and the conditions of the experimental tests.

Appendix A. Supplementary material

Supplementary data to this article can be found online at https://doi.org/10.1016/j.enconman.2023.117070.

References

[1] Masson-Delmotte V, Zhai P, Pirani A, Connors SL, Péan C, Berger S, et al. Summary for Policymakers. Sixth Assessment Report of the Intergovernmental Panel on Climate Change (IPCC). 2021.
[2] Zachl A, Buchmayr M, Gruber J, Anca-Couce A, Scharler R, Hochenauer C. Shifting of the flame front in a small-scale commercial downdraft gasifier by water injection and exhaust gas recirculation. Fuel 2021;303:121297. https://doi.org/10.1016/j.fuel.2021.121297.
[3] Pongratz G, Subotić V, von Berg L, Schroettner H, Hochenauer C, Martini S, et al. Real coupling of solid oxide fuel cells with a biomass steam gasifier: Operating boundaries considering performance, tar and carbon deposition analyses. Fuel 2022;316:123310. https://doi.org/10.1016/j.fuel.2022.123310.
[4] Molino A, Chianese S, Musmarra D. Biomass gasification technology: The state of the art overview. J Energy Chem 2016;25:10–25. https://doi.org/10.1016/j.jechem.2015.11.005.
[5] Anca-Couce A, Hochenauer C, Scharler R. Bioenergy technologies, uses, market and future trends with Austria as a case study. Renew Sustain Energy Rev 2021;135:110237. https://doi.org/10.1016/j.rser.2020.110237.
[6] Karl J, Pröll T. Steam gasification of biomass in dual fluidized bed gasifiers: A review. Renew Sustain Energy Rev 2018;98:64–78. https://doi.org/10.1016/j.rser.2018.09.010.
[7] Schmid JC, Benedikt F, Fuchs J, Mauerhofer AM, Müller S, Hofbauer H. Syngas for biorefineries from thermochemical gasification of lignocellulosic fuels and residues—5 years' experience with an advanced dual fluidized bed gasifier design. Biomass Convers Biorefin 2021;11(6):2405–42. https://doi.org/10.1007/s13399-019-00486-2.
[8] Larsson A, Kuba M, Berdugo Vilches T, Seemann M, Hofbauer H, Thunman H. Steam gasification of biomass – Typical gas quality and operational strategies derived from industrial-scale plants. Fuel Process Technol 2021;212:106609. https://doi.org/10.1016/J.FUPROC.2020.106609.
[9] Luo H, Wang X, Liu X, Wu X, Shi X, Xiong Q. A review on CFD simulation of biomass pyrolysis in fluidized bed reactors with emphasis on particle-scale models. J Anal Appl Pyrolysis 2022;162:105433. https://doi.org/10.1016/j.jaap.2022.105433.
[10] Gómez-Barea A, Leckner B. Modeling of biomass gasification in fluidized bed. Prog Energy Combust Sci 2010;36:444–509. https://doi.org/10.1016/j.pecs.2009.12.002.
[11] Adamczyk WP. Application of the numerical techniques for modelling fluidization process within industrial scale boilers. Arch Comput Methods Eng 2017;24:669–702. https://doi.org/10.1007/s11831-016-9186-z.
[12] Yang S, Wang H, Wei Y, Hu J, Wei J. Particle-scale modeling of biomass gasification in the three-dimensional bubbling fluidized bed. Energy Convers Manag 2019;196:1–17. https://doi.org/10.1016/j.enconman.2019.05.105.
[13] Klimanek A, Adamczyk W, Katelbach-Woźniak A, Węcel G, Szlęk A. Towards a hybrid Eulerian-Lagrangian CFD modeling of coal gasification in a circulating fluidized bed reactor. Fuel 2015;152:131–7. https://doi.org/10.1016/j.fuel.2014.10.058.
[14] Schneiderbauer S, Kinaci ME, Hauzenberger F. CFD simulation of iron ore reduction in industrial-scale fluidized beds. Steel Res Int 2020. https://doi.org/10.1002/srin.202000232.
[15] von Berg L, Soria-Verdugo A, Hochenauer C, Scharler R, Anca-Couce A. Evaluation of heat transfer models at various fluidization velocities for biomass pyrolysis conducted in a bubbling fluidized bed. Int J Heat Mass Transf 2020;160:120175.
[16] Safarian S, Unnþórsson R, Richter C. A review of biomass gasification modelling. Renew Sustain Energy Rev 2019;110:378–91. https://doi.org/10.1016/J.RSER.2019.05.003.
[17] Alobaid F, Almohammed N, Massoudi Farid M, May J, Rößger P, Richter A, et al. Progress in CFD simulations of fluidized beds for chemical and energy process engineering. Prog Energy Combust Sci 2022;91:100930. https://doi.org/10.1016/j.pecs.2021.100930.
[18] Ostermeier P, Fischer F, Fendt S, DeYoung S, Spliethoff H. Coarse-grained CFD-DEM simulation of biomass gasification in a fluidized bed reactor. Fuel 2019;255:115790. https://doi.org/10.1016/j.fuel.2019.115790.
[19] Yang S, Wang S, Wang H. Numerical study of biomass gasification in a 0. 3 MW th full-loop circulating fluidized bed gasifier. Energy Convers Manag 2020;223:113439. https://doi.org/10.1016/j.enconman.2020.113439.
[20] Kraft S, Kirnbauer F, Hofbauer H. CPFD simulations of an industrial-sized dual fluidized bed steam gasification system of biomass with 8 MW fuel input. Appl Energy 2017;190:408–20. https://doi.org/10.1016/J.APENERGY.2016.12.113.
[21] Lu L, Gao X, Dietiker JF, Shahnam M, Rogers WA. MFiX based multi-scale CFD simulations of biomass fast pyrolysis: A review. Chem Eng Sci 2022;248:117131. https://doi.org/10.1016/j.ces.2021.117131.
[22] Anca-Couce A, Zobel N. Numerical analysis of a biomass pyrolysis particle model: Solution method optimized for the coupling to reactor models. Fuel 2012;97:80–8. https://doi.org/10.1016/J.FUEL.2012.02.033.
[23] Gao X, Yu J, Lu L, Rogers WA. Coupling particle scale model and SuperDEM-CFD for multiscale simulation of biomass pyrolysis in a packed bed pyrolyzer. AIChE J 2021;67:1–15. https://doi.org/10.1002/aic.17139.
[24] Gao Xi, Lu L, Shahnam M, Rogers WA, Smith K, Gaston K, et al. Assessment of a detailed biomass pyrolysis kinetic scheme in multiscale simulations of a single-particle pyrolyzer and a pilot-scale entrained flow pyrolyzer. Chem Eng J 2021;418:129347. https://doi.org/10.1016/j.cej.2021.129347.
[25] von Berg L, Anca-Couce A, Hochenauer C, Scharler R. Multi-scale modelling of fluidized bed biomass gasification using a 1D particle model coupled to CFD. Fuel 2022;324:124677. https://doi.org/10.1016/j.fuel.2022.124677.
[26] Liu H, Cattolica RJ, Seiser R. CFD studies on biomass gasification in a pilot-scale dual fluidized-bed system. Int J Hydrogen Energy 2016;41:11974–89. https://doi.org/10.1016/j.ijhydene.2016.04.205.
[27] Blehrmühlhuber M. CFD Simulation of Hydrodynamics in Fluidized Beds. Master Thesis, TUG 2018.
[28] Shadle L, Guenther C, Cocco R, Panday R. NETL Challenge Problem III (2010): NETL's Circulating Fluidized Bed (CFB) and PSRI's Bubbling Fluid Bed (BFB) 2010. https://mfix.netl.doe.gov/experimentation/challenge-problems.
[29] Anca-Couce A, Sommersacher P, Scharler R. Online experiments and modelling with a detailed reaction scheme of single particle biomass pyrolysis. J Anal Appl Pyrolysis 2017;127:411–25. https://doi.org/10.1016/j.jaap.2017.07.008.
[30] Gidaspow D, Bezburuah R, Ding J. Hydrodynamics of circulating fluidized beds: Kinetic theory approach. Proc 7th Eng Found Conf Fluid 1992.
[31] ANSYS Fluent. Theory Guide 2021 R2 2021.
[32] Cloete S, Johansen ST, Amini S. Grid independence behaviour of fluidized bed reactor simulations using the two fluid model: effect of particle size. Powder Technol 2015;269:153–65. https://doi.org/10.1016/j.powtec.2014.08.055.
[33] Cloete S, Cloete JH, Amini S. Comparison of the filtered two fluid model and dense discrete phase model for large-scale fluidized bed reactor simulations. Part Technol Forum 2016 - Core Program Area 2016 AIChE Annu Meet 2016:516–23.
[34] Milioli CC, Milioli FE, Holloway W, Agrawal K, Sundaresan S. Filtered two-fluid models of fluidized gas-particle flows: new constitutive relations. AIChE J 2013;59:3265–75. https://doi.org/10.1002/aic.14130.
[35] Igci Y, Sundaresan S. Constitutive models for filtered two-fluid models of fluidized gas-particle flows. Ind Eng Chem Res 2011;50:13190–201. https://doi.org/10.1021/ie200190q.
[36] Schneiderbauer S, Pirker S. Filtered and heterogeneity-based subgrid modifications for gas–solid drag and solid stresses in bubbling fluidized beds. AIChE J 2014;60:839–54. https://doi.org/10.1002/aic.14321.
[37] Tricomi L, Melchiori T, Chiaramonti D, Boulet M, Lavoie JM. Numerical investigation of a cold bubbling bed throughout a dense discrete phase model with KTGF collisional closure. Biofuels Eng 2018;2:32–50. https://doi.org/10.1515/bfuel-2017-0003.
[38] ANSYS Fluent. Users Guide 2021 R2 2021.
[39] Scharler R, Gruber T, Ehrenhöfer A, Kelz J, Bardar RM, Bauer T, et al. Transient CFD simulation of wood log combustion in stoves. Renew Energy 2020;145:651–62. https://doi.org/10.1016/J.RENENE.2019.06.053.
[40] Mellin P, Kantarelis E, Yang W. Computational fluid dynamics modeling of biomass fast pyrolysis in a fluidized bed reactor, using a comprehensive chemistry scheme. Fuel 2014;117:704–15. https://doi.org/10.1016/J.FUEL.2013.09.009.
[41] Hou K, Hughes R. The kinetics of methane steam reforming over a Ni/α-Al2O catalyst. Chem Eng J 2001;82:311–28. https://doi.org/10.1016/S1385-8947(00)00367-3.
[42] Van den Aarsen FG. Fluidised bed wood gasifier performance and modeling. Enschede (Netherlands): Technische Hogeschool Twente; 1985.
[43] Dupont C, Boissonnet G, Seiler JM, Gauthier P, Schweich D. Study about the kinetic processes of biomass steam gasification. Fuel 2007;86:32–40. https://doi.org/10.1016/j.fuel.2006.06.011.
[44] Anca-Couce A, Caposciutti G, Gruber T, Kelz J, Bauer T, Hochenauer C, et al. Single large wood log conversion in a stove: experiments and modelling. Renew Energy 2019;143:890–7.
[45] Van de steene L, Tagutchou JP, Escudero Sanz FJ, Salvador S. Gasification of woodchip particles: Experimental and numerical study of char-H2O, char-CO2, and char-O2 reactions. Chem Eng Sci 2011;66(20):4499–509. https://doi.org/10.1016/j.ces.2011.05.045.
[46] Ranzi E, Cuoci A, Faravelli T, Frassoldati A, Migliavacca G, Pierucci S, et al. Chemical kinetics of biomass pyrolysis. Energy Fuel 2008;22(6):4292–300. https://doi.org/10.1021/ef800551t.
[47] Agarwal PK. Transport phenomena in multi-particle systems—IV. Heat transfer to a large freely moving particle in gas fluidized bed of smaller particles. Chem Eng Sci 1991;46:1115–27. https://doi.org/10.1016/0009-2509(91)85104-6.

[48] Hayhurst AN, Parmar MS. Measurement of the mass transfer coefficient and sherwood number for carbon spheres burning in a bubbling fluidized bed. Combust Flame 2002;130:361–75. https://doi.org/10.1016/S0010-2180(02)00387-5.
[49] Liu H, Cattolica RJ, Seiser R. Operating parameter effects on the solids circulation rate in the CFD simulation of a dual fluidized-bed gasification system. Chem Eng Sci 2017;169:235–45. https://doi.org/10.1016/j.ces.2016.11.040.
[50] ANSYS. Lecture 5: Particulate Flows Multiphase Modeling using ANSYS Fluent 2015.
[51] Cloete S, Johansen ST, Braun M, Popoff B, Amini S. Evaluation of a Lagrangian Discrete Phase Modeling Approach for Application To Industrial Scale Bubbling Fluidized Beds. Proc 10th Int Conf Circ Fluid Beds Fluid Technol - CFB-10 2011;7:1–8.
[52] Syamlal M, Rogers W, O'Brien TJ. MFIX documentation theory guide n.d. https://doi.org/10.2172/10145548.
[53] Lun CKK, Savage SB, Jeffrey DJ, Chepurniy N. Kinetic theories for granular flow: inelastic particles in Couette flow and slightly inelastic particles in a general flowfield. J Fluid Mech 1984;140:223–56. https://doi.org/10.1017/S0022112084000586.
[54] Schaeffer DG. Instability in the evolution equations describing incompressible granular flow. J Differ Equ 1987;66:19–50. https://doi.org/10.1016/0022-0396(87)90038-6.
[55] Johnson PC, Jackson R. Frictional–collisional constitutive relations for granular materials, with application to plane shearing. J Fluid Mech 1987;176:67–93. https://doi.org/10.1017/S0022112087000570.
[56] Ahmadi G, Ma D. A thermodynamical formulation for dispersed multiphase turbulent flows—1: Basic theory. Int J Multiph Flow 1990;16:323–40. https://doi.org/10.1016/0301-9322(90)90062-N.
[57] Benedikt F, Kuba M, Schmid JC, Müller S, Hofbauer H. Assessment of correlations between tar and product gas composition in dual fluidized bed steam gasification for online tar prediction. Appl Energy 2019;238:1138–49. https://doi.org/10.1016/j.apenergy.2019.01.181.
[58] Aghaalikhani A, Schmid JC, Borello D, Fuchs J, Benedikt F, Hofbauer H, et al. Detailed modelling of biomass steam gasification in a dual fluidized bed gasifier with temperature variation. Renew Energy 2019;143:703–18.
[59] Benedikt F, Schmid JC, Fuchs J, Mauerhofer AM, Müller S, Hofbauer H. Fuel flexible gasification with an advanced 100 kW dual fluidized bed steam gasification pilot plant. Energy 2018;164:329–43. https://doi.org/10.1016/j.energy.2018.08.146.
[60] Cloete JH, Cloete S, Radl S, Amini S. Evaluation of wall friction models for riser flow. Powder Technol 2016;303:156–67. https://doi.org/10.1016/j.powtec.2016.07.009.
[61] Gómez-Barea A, Ollero P, Leckner B. Optimization of char and tar conversion in fluidized bed biomass gasifiers. Fuel 2013;103:42–52. https://doi.org/10.1016/j.fuel.2011.04.042.
[62] Kraft S, Kuba M, Hofbauer H. The behavior of biomass and char particles in a dual fluidized bed gasification system. Powder Technol 2018;338:887–97. https://doi.org/10.1016/j.powtec.2018.07.059.
[63] Wang X, Kersten SRA, Prins W, Van Swaaij WPM. Biomass pyrolysis in a fluidized bed reactor. Part 2: Experimental validation of model results. Ind Eng Chem Res 2005;44:8786–95. https://doi.org/10.1021/ie050486y.
[64] Kersten SRA, Wang X, Prins W, Van Swaaij WPM. Biomass pyrolysis in a fluidized bed reactor. Part 1: Literature review and model simulations. Ind Eng Chem Res 2005;44:8773–85. https://doi.org/10.1021/ie0504856.
[65] Zhang R, Ku X, Yang S. Study of air-steam gasification of spherocylindrical biomass particles in a fluidized bed by using CFD-DEM coupling with the multi-sphere model. Energy Convers Manage 2023;276:116561. https://doi.org/10.1016/j.enconman.2022.116561.